11th Asia-Pacific Conference on Combustion,
The University of Sydney, NSW Australia
10th -14th December 2017.

Combustion Measurements of Waste Cooking Oil Biodiesel

C. Ming[1], I.M.R. Fattah[1], Q.N Chan[1], P.R. Medwell[2], S. Kook[1], E.R. Hawkes[1], G.H. Yeoh[1]

[1]School of Mechanical and Manufacturing Engineering

UNSW Sydney, NSW 2052, Australia

[2]School of Mechanical Engineering

The University of Adelaide, SA 5005, Australia

Abstract

An experimental investigation was performed to assess the combustion characteristics of a waste cooking oil (WCO) biodiesel fuel under simulated compression-ignition engine conditions. A conventional diesel was used as a base fuel for comparison purpose. The fuels were injected into the quiescent steady environment inside a constant-volume combustion chamber (CVCC) of 19.4 kg/m^3 ambient density, 6 MPa ambient pressure, and 1100 K bulk temperature. A range of optical diagnostics were performed, to compare the fuels over ambient O_2 concentrations of 10-21 vol.%, and injection pressures of 70-130 MPa. The results reveal that for the investigated test conditions (i) the lift-off lengths and the first soot distances of the biodiesel are consistently longer than that of diesel; (ii) the peak soot level of the flame increases with the relative distance between the first soot formation and flame lift-off; and (iii) the WCO biodiesel has a lower soot formation propensity than diesel. The fuel liquid lengths were also measured to be shorter than their lift-off distances, indicating no interaction between their spray and combustion processes.

1 Introduction

Biodiesels are mixtures of fatty acid methyl esters (FAMEs) with differing chain lengths and degrees of saturation, which can vary significantly depending on their feedstocks [1]. Biodiesel fuels contain oxygen, which have been reported to provide an effective route to enhance combustion, and to reduce soot formation in compression-ignition engines [2]. Nonetheless, biodiesels have physical and chemical properties that are different to that of conventional diesel. These differences in fuel properties can have a complicated impact on the fuel atomization, evaporation, combustion and soot formation processes, and hence, the ensuing engine performance [3].

This work is aimed at assessing the combustion properties of a biodiesel from the transesterification of waste cooking oil (WCO) under simulated compression-ignition engine conditions in a constant-volume combustion chamber (CVCC). Experiments are performed under three different ambient O_2 concentrations of 10, 15 and 21 vol.%, which are used to simulate different exhaust gas recirculation levels. The experiments are performed under fixed ambient density, pressure and temperature values of 19.4 kg/m^3, 6 MPa and 1100 K, respectively. The experiments are also assessed over three injection pressures of 70, 100 and 130 MPa. OH chemiluminescence and high-speed flame natural luminosity imaging are used to assess impact of these varied parameters on the air entrainment rate occurring upstream of the lift-off length, and the downstream soot formation and combustion processes of the biodiesel jet flame. To provide context to the examination, comparative measurements using a conventional diesel are also performed.

2 Experimental Details

Experiments were performed in an optically-accessible CVCC under simulated, quiescent diesel engine conditions. The CVCC has a 114 × 114 × 114 mm cubical combustion chamber, six window ports, and eight access ports for instrumentations and valves. For this work, sapphire windows were installed at four sides of the chamber to enable optical access. A diesel injector was mounted at the centre of a metal side port so that the fuel spray was directed into the centre of the chamber. An agitator was mounted at the top of the CVCC and was used to maintain a spatially uniform temperature environment. A schematic of the CVCC configuration along with the diagnostic set-ups used is shown in Fig. 1. The operation of the chamber was initiated by filling up the chamber with a premixed, lean combustible charge (*e.g.* acetylene, hydrogen, nitrogen and oxygen). The mixture was subsequently ignited with a spark plug to create a high temperature and pressure environment inside the chamber. Following the premixed combustion, the combustion products cooled over a relatively long time (~8 s) due to heat transfer to the chamber walls, the vessel pressure, therefore, decreased correspondingly. When the targeted pressure was reached, the injector was triggered and the fuel injection, auto-ignition and combustion processes ensued. The test conditions for the experiments are summarized in Table 1. The fuel injection system used comprised of a low pressure fuel

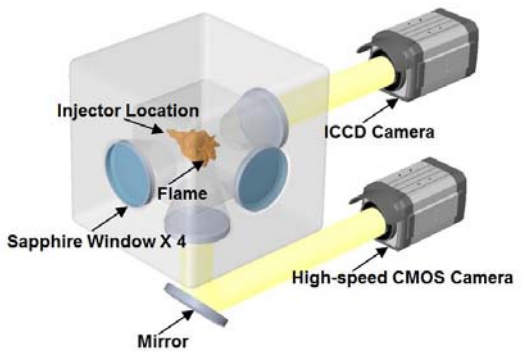

Figure 1: Schematic of experimental arrangement including the combustion vessel, OH-chemiluminescence and high-speed natural luminosity imaging setups.

pump a high pressure fuel pump, a Bosch commercial common-rail system (CP4) and an axially drilled single-hole solenoid injector with an orifice diameter of 105 µm. A common-rail PCV driver (Zenobalti, ZB-1200) was used to regulate and maintain the injection pressure, whilst an injector driver (Zenobalti, ZB-5100) was used to control the injection system to deliver the required fuel mass. A summary of the injection conditions used is provided in Table 1. For this work, comparative measurements were performed between a WCO biodiesel and a conventional diesel. The WCO biodiesel has higher fuel density and viscosity values when compared with diesel. It is noted that for the injection conditions used in this work, the difference in the actual injected mass of the biodiesel and diesel, when measuring with a Bosch tube type injection rate meter, was found to be within experimental errors of the injection rate meter across the varied conditions. The same injection parameters were therefore applied to both fuels, for all experiments. Gas-chromatography and mass-spectrometry (GCMS) was performed on the fuels. WCO biodiesel, is found to comprise mainly of FAMEs with long carbon chains such as oleic, linoleic and linolenic acids, and is oxygenated (11 wt%). The biodiesel therefore has a lower heating value and a higher stoichiometric mixture fraction than diesel. From the fuel specifications data that were provided by the fuel supplier, the biodiesel is also reported to have a higher cetane number than diesel. A summary of the main fuel properties of WCO biodiesel and diesel is provided in Table 2.

The optical combustion diagnostics used for this work, including intensified OH chemiluminescence imaging using an intensified CCD (ICCD) camera, and flame natural luminosity imaging with a high-speed CMOS camera. The cameras were arranged for viewing through the side or bottom windows of the CVCC, as depicted in Fig. 1, and were applied simultaneous to image the same injection event. For the OH-chemiluminescence imaging, the light emission from flame was detected through a 10 nm bandwidth interference filter (centred at 310 nm), using the ICCD camera (Andor iStar) that was fitted with a 50-mm f#3.5 UV lens. The camera was triggered to open for 2.5 ms after the quasi-steady lift-off length of the flame was established, and was stopped before the end of injection. A typical OH-chemiluminescence image recorded is shown in Fig. 2. In this figure, the injector orifice is located at the left edge of the image. The diesel fuel was injected from left to right at 100 MPa injection pressure and 15% ambient oxygen concentration by an injector equipped with a nozzle with an orifice diameter of 105 µm. The ambient pressure and temperature were maintained to be 6 MPa and 1100 K during the injection. For the high-speed flame luminosity imaging, a CMOS camera (Photron SA5) equipped with a 85-mm f#1.8 lens, was operated at a frame rate of 15,000 frames per second (fps) was used. The CMOS camera was synchronized to the start of injection of the injector, and 100 images were captured for each run. A typical instantaneous flame luminosity image captured for the same diesel jet flame presented in Fig. 3, but at 2 ms after start of injection (aSOI), is shown in Fig. 4. The diesel fuel was injected from the top to bottom in this image. It is noted that at least five runs were performed for each measurement to ensure good repeatability.

Test conditions	
Ambient oxygen concentration (vol.%)	10, 15, 21
Ambient gas density (kg/m^3)	19.4
Ambient pressure (MPa)	6
Bulk temperature (K)	1100
Injection conditions	
Nozzle diameter (µm)	105
Injection pressure (MPa)	70, 100, 130
Injection quantity (mg)	10

Table 1: Summary of test and injection conditions.

Main properties		
Properties	WCO	Diesel
Density (kg/m^3)	883	832
Viscosity (@ 293 K, mm^2/s)	4.6	3.2
Oxygen content (wt%)	11	0
Higher HV (MJ/kg)	40.8	43.4
Stoichiometric air-fuel ratio (AFR) by mass	12.73	14.5
Cetane number	53.2	51

Table 2: Main fuel properties of waste cooking oil (WCO) biodiesel and diesel.

3 Results and Discussion

Flame structural information, including flame lift-off and first soot distance from the nozzle, during its mixing-controlled combustion phase has been shown to be critical towards the understanding of soot formation process [4]. The flame lift-off length, which refers to the distance from the fuel injector nozzle to where the flame stabilizes, is indicative of the location where intense combustion reaction of the flame initiates [5], and is widely used to characterize the amount of fuel-air premixing occurring upstream of the lift-off [6]. The first soot distance, on the other hand, refers to the distance from the injector to the location where intense flame luminosity is first detected and is used to indicate the initial onset of soot in the flame [6]. The lift-off lengths of the flames were derived from their time-averaged OH chemiluminescence images, following the approaches that were detailed in Ref. [5]. In brief, the lift-off length value was determined by finding the distance between the injector and first axial location where chemiluminescence intensity of the flame exceeded ~50% of the levelling-off value, as is shown in Fig. 2. The first soot distances, on the other hand, were derived from the high-speed natural flame luminosity images that were captured using the high-speed camera. The images were first corrected for background, dark charge and detector attenuation, and were subsequently binarized to enable logical operations [7, 8]. The first soot distance was determined by measuring the minimum distance from the injector to the location where half of the pixels on an arc with a spreading angle of $\Theta/2$ are occupied by

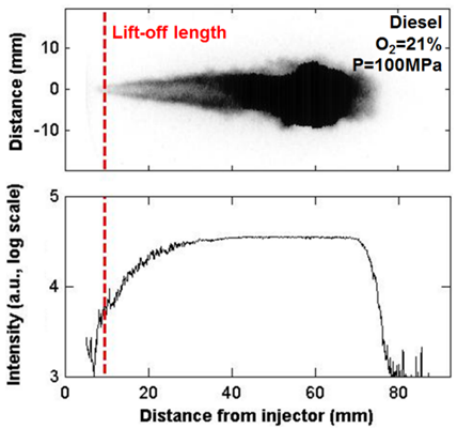

Figure 2: An example of the time-averaged OH-chemiluminescence emission image at 310 nm (top) and its axial intensity profile (bottom). Diesel was injected at 15 vol.% ambient oxygen concentration and 100 MPa injection pressure by a fuel injector with 105 µm nozzle orifice diameter.

the binarized flame area. This definition was used to minimize the sensitivity of the first soot distance calculations to the threshold setting used or potential fluctuations in the binarized flame area. It is noted that the flame central axis was taken as the line from the injector tip through to the centroid of the flame area, whilst flame spreading angle was defined as the average flame spreading angle between a starting and ending points along the flame central axis. The starting and ending points were set to be 45% and 55% of the instantaneous flame length for this work.

The averaged lift-off lengths and the first soot distances of the diesel and WCO biodiesel are plotted as a function of injection pressure, for the test conditions with ambient O_2 concentration of 10, 15 and 21 vol.%, in Fig. 4. From Fig. 4, it can be seen that lift-off lengths of the flames are found to increase with increasing injection pressure or decreasing ambient O_2 concentration. It is noted that previous studies have shown that an increase in injection pressure would result in higher velocity in spray, which would push the initial combustion zone of the flame downstream [9]. A reduction in ambient O_2 concentration, on the other hand, has been shown to necessitate a greater entrainment of total ambient gas with smaller fraction of oxygen (hence, longer mixing time) before combustion reactions can take place [10]. The current results are therefore consistent with the previously observed trends in lift-off lengths with respect to injection pressure and oxygen concentration effects. From Fig. 4, it can be observed that that the lift-off lengths of the WCO biodiesel flames are consistently higher than that of diesel flames. Previous studies have demonstrated flame lift-off is affected by the ignition quality of its fuel, which in turn, is correlated to its physical and chemical properties. From Table 2, it can be seen that the cetane number of the WCO biodiesel (*i.e.* 53.2), albeit slightly higher, is comparable to that of diesel (*i.e.* 51). The viscosity of the WCO biodiesel, on the other hand, is greater than that of diesel. Previous studies have reported that a high viscosity can impact on the atomization, vaporization and fuel-air mixing processes of the fuel. This can lead to a prolonged time between the beginning of fuel injection and the start of combustion process [11], which would subsequently impact on its ignition quality. Further investigation, however, is required to elucidate and extend the observed results. It should be noted that the liquid lengths of the WCO biodiesel and diesel were measured to be ~8.7 mm and ~7.7 mms, respectively, when diffused back illumination technique was applied by the authors. The longer liquid length observed for WCO biodiesel is expected because of its higher heat of vaporization due the presence of FAMEs with longer carbon chains [12]. The shorter liquid lengths of the fuels, when compared with their lift-off lengths, imply that there is no interplay between the spray and combustion processes for the fuels, under the investigated conditions.

In previous studies, it has been shown the soot inception time of a jet flame can be approximated from the observed location of the first soot formation relative to the flame lift-off [6]. This distance of lift-off length to soot formation region, which is termed as soot formation distance in the subsequent discussion, has been shown to depend strongly on fuel type, such that a longer distance is observed for fuel with lower soot formation tendency [4, 6]. In Fig. 5, the soot formation distances of the WCO biodiesel and diesel jet flames are plotted as a function of injection pressure and ambient O_2 concentration. The peak spatially integrated natural luminosity (SINL) values of the WCO and diesel flames under different test conditions are also computed and are presented in Fig. 5. It is acknowledged that the SINL signal, which was calculated by summing up the intensities of all pixels of each image, is a complex function of the soot concentration, properties and temperature [13]. Nonetheless, the peak SINL has been widely shown to be useful in providing a relative measure of the soot content of sooty flames, and is therefore used here to rank-order the soot level of the diesel and WCO biodiesel flames. In Fig. 5, it can be seen that a higher peak SINL value/soot content is observed for flame with shorter soot formation distance. From the figure, it can also be observed that under the same test and injection

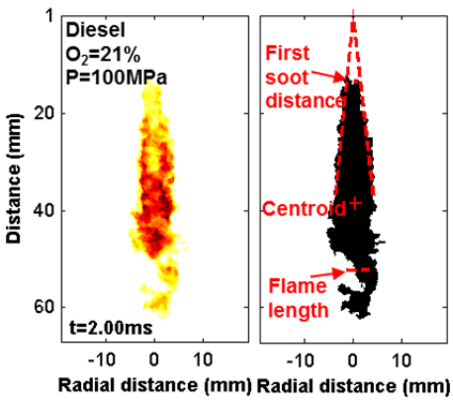

Figure 3: A typical instantaneous flame luminosity image of a diesel spray flame, recorded at 2 ms aSOI (left). The same flame image after background, dark charge and detector attenuation correction (right). The parameters of interest of the flame were derived from the boundary of the resulting image. Definitions of centroid, flame length and first soot distance are shown in the figure.

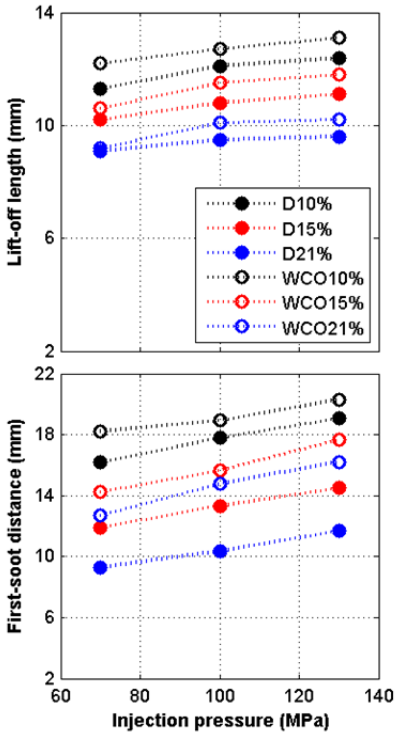

Figure 4: Comparisons of the lift-off lengths (top) and the first soot distance (bottom) of diesel and WCO jet flames. The lift-off lengths and the first soot distances are plotted as a function of injection pressure for three selected ambient oxygen concentrations of 10, 15 and 21 vol.%.

conditions, the soot formation distance of WCO biodiesel flame is consistently longer than that of diesel. As is noted in Table 2, the WCO biodiesel is oxygenated whereas the diesel fuel is not. The oxygen content of the biodiesel increases the critical mixture fraction for soot formation limit of biodiesel in relation to diesel [4]. It can therefore be expected that a smaller percentage of the biodiesel fuel jet mixtures would exceed its soot formation limit, and therefore, less downstream soot would form. The fuel molecular structure and composition of the WCO biodiesel are also less prone to soot formation than diesel. The WCO biodiesel contains carbon-oxygen bonds that are harder to break. This will hinder the formation of carbon-carbon double and triple bonds that can lead to the formation of soot precursors, and ultimately soot [4]. From the GCMS analysis that was performed (not shown here), the diesel used was found to contain aromatic compounds such as toluene, xylene and ethyl-toluene, which have strong tendencies to form soot during combustion, whereas the WCO used is aromatic-free. The fuel oxygenation, molecular structure and fuel composition effects of the WCO biodiesel, in combined with its longer observed lift-off length, would therefore contribute towards its observed lower peak SINL/soot content, when compared with diesel.

From Fig. 5, it can be seen that the soot formation distance for both WCO biodiesel and diesel increase with increasing injection pressure for both fuels. Different trends, however, are observed for the fuels across the varied ambient O_2 concentration. Specifically, the soot formation distance of diesel is found to decrease monotonically with increasing ambient O_2 concentration. The soot formation distance of WCO biodiesel, on the other hand, is observed to first decrease and then increase as the ambient O_2 concentration increases from 10% to 21%. It is noted that similar trends were also observed in a previous study [14] that was performed to examine the effects of ambient oxygen concentration on WCO biodiesel and diesel spray combustion. In their study, it was suggested that the soot formation of the WCO biodiesel was maintained without sufficient oxidation, when the ambient O_2 concentration decreases from 21% to 15%, which resulted in an increased soot yield for the biodiesel. Further investigation, however, is required to confirm this.

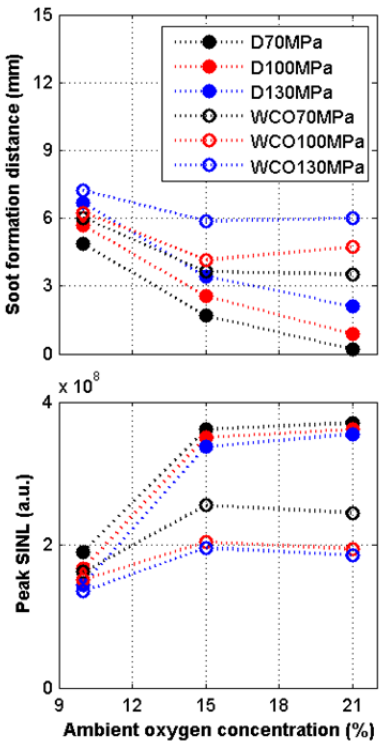

Figure 5: Comparisons of the soot formation distances (top) and the peak SINL (bottom) of diesel and WCO jet flames. The soot formation distances and the peak SINL are plotted as a function of ambient oxygen concentration for three selected injection pressures (70, 100 and 130 MPa).

4 Conclusion

Experiments were performed in an optically-accessible constant-volume combustion chamber (CVCC) at ambient conditions that are representative of compression-ignition engine (19.4 kg/m^3 ambient density, 6 MPa ambient pressure, 1100 K bulk temperature, 10-21 vol.% ambient O_2 concentrations, 70-130 MPa injection pressure), comparing waste cooking oil (WCO) biodiesel to conventional diesel. The results reveal that for the investigated experimental conditions, the lift-off lengths and the first soot distances of the biodiesel were consistently longer than that of diesel. The peak soot level of the flame was observed to correspond to the distance from the lift-off length to the location of the first soot formation. The WCO biodiesel flames were found to have lower soot content than diesel, under the same test and injection conditions. The liquid lengths of both fuels were measured to be shorter than their lift-off lengths; implying interaction between the spray and combustion processes of the fuels was not significant.

References

[1] C.J. Chuck, C.D. Bannister, J.G. Hawley, M.G. Davidson, I. La Bruna, A. Paine, Energy 23 (2009) 2290-2294.

[2] X. Wang, Z. Huang, O.A. Kuti, W. Zhang, K. Nishida, Proc. Combust. Inst 33 (2011) 2071-2077.

[3] S.K. Hoekman, A. Broch, C. Robbins, E. Ceniceros, M. Natarajan, Renew. Sustain. Energy Rev 16 (2011) 143–169.

[4] J. G. Nerva, C. L. Genzale, S. Kook, J. M. Garcia-Oliver, L. M. Pickett, Int. J. Engine Res. 14 (2012) 373-390.

[5] B. Higgins, D.L. Siebers, SAE Paper 2001-01-0918 (2001).

[6] L.M. Pickett, D.L. Siebers, Int. J. Engine Res 7 (2005) 103-130.

[7] Q. N. Chan, P. R. Medwell, G. J. Nathan, Exp. Fluids 55 (2014).

[8] N.H. Qamar, G.J. Nathan, Z.T. Alwahabi, Q.N. Chan, Combust. Flame 158 (2011) 2458-2464.

[9] D.L. Siebers, B. Higgins, SAE Paper 2001-01-0530 (2001).

[10] D.L. Siebers, B. Higgins, L.M. Pickett, SAE Paper 2002-01-0890 (2002).

[11] M. Shahabuddin, A.M. Liaquat, H.H. Masjuki, M.A. Kalam, M. Mofijur, Renew. Sustainable Energy Rev. 21 (2013), 623-632.

[12] D.L. Siebers, SAE Paper 980809 (1998).

[13] C.J. Polonowski, C.J. Mueller, C.R. Gehrke, T. Bazyn, G.C. Martin, P.M. Lilo, SAE Paper 2011-01-1812 (2011).

[14] J. Zhang, W. Jing, W. L. Roberts, T. Fang, Energy 57 (2013) 722-732.